In order to match the observations at large distances from the nucleus, we have, in the next order of model improvement, followed Bertaux *et al.* (*5*). In this scheme, the atoms again flow outward from a point source, but with a thermal dispersion about the radial velocity. Charge exchange with solar wind protons is included as the principal loss process. Figure 5 shows the results computed with this model for a mean velocity of 8 km sec^{-1} and the values of g and a given above. The effect of radiation pressure is to produce elliptical, rather than circular, outer isophotes. Theoretical contours are shown for infinite and 5.3-day lifetimes to demonstrate the effects of the loss mechanism. The best fit was for the infinite lifetime case, rather than the 5.3-day lifetime which fit the Bennett data. The longer lifetime is probably due to differences in solar wind intensity. Part of the effect may also be due to a high-velocity component in the velocity distribution of the escaping hydrogen. The production rate derived from this model was 3.6×10^{28} atom sec^{-1} $ster^{-1}$, the same as that derived from the first-order theory.

For comparison, a production rate derived from the OGO-5 data on Comet Bennett was about 6×10^{28} atom sec^{-1} $ster^{-1}$ when the comet was 0.8 A.U. from the sun (*4*, *5*). If one assumes an inverse square law dependence of production rate on sun-comet distance, then the production rate for Bennett at the sun-comet distance of these observations was some six times greater than the production rate for Kohoutek.

C. B. OPAL
G. R. CARRUTHERS
D. K. PRINZ
R. R. MEIER
U.S. Naval Research Laboratory, Washington, D.C. 20375

References and Notes

1. G. R. Carruthers and T. L. Page, *Science* **177**, 788 (1972); G. R. Carruthers, *Appl. Opt.* **12**, 2501 (1973).
2. P. D. Feldman, P. Z. Takacs, W. G. Fastie, B. Donn, *Science* **185**, 705 (1974).
3. A. D. Code, T. E. Houck, C. F. Lillie, *NASA SP-310* (1972), p. 109.
4. H. U. Keller, *Astron. Astrophys.* **27**, 51 (1973).
5. J. L. Bertaux, J. E. Blamont, M. Festou, *ibid.* **25**, 415 (1973).
6. We are grateful to the Sounding Rocket Division of the National Aeronautics and Space Administration for supplying and providing field support for the rocket. The Air Force Avionics Laboratory provided much of the funding to build the payload. We thank U. Keller and P. Feldman for helpful discussions. H. Merchant and D. King assisted in the preparation of the payload.

22 April 1974

Rocket Ultraviolet Spectrophotometry of Comet Kohoutek (1973f)

Abstract. *Observations of Comet Kohoutek (1973f) in the spectral region between 1200 and 3200 angstroms were made from an Aerobee rocket on 5.1 January 1974 universal time. The strongest features observed were the Lyman alpha line of neutral atomic hydrogen at 1216 angstroms and the hydroxyl (OH) bands at 3090 and 3142 angstroms. Atomic oxygen and atomic carbon were also detected, and their luminosity implies a production rate (of carbon monoxide or carbon dioxide) commensurate with that of water vapor.*

An Aerobee 200 rocket carrying two spectrophotometers was launched from White Sands Missile Range (New Mexico) at 0145 U.T. on 5 January 1974 to study the ultraviolet emissions from Comet Kohoutek (1973f) in the spectral range 1200 to 3200 Å. At the time of launch, the comet-sun-earth angle was 20.3° and the sun was 5° below the rocket horizon at apogee (232 km). Scattered sunlight near the horizon made it difficult for the star tracker of the attitude control system to lock on the comet, whose magnitude was estimated visually at $m_V \approx +2.5$, approximately three magnitudes weaker than predicted. Nevertheless, several seconds of data on the coma were obtained, and observations of the tail were obtained during rocket descent after the star tracker locked on when the solar depression angle exceeded 7°.

In addition to the Lyman α line of atomic hydrogen (HI) at 1216 Å and the (0, 0) and (1, 1) bands of OH at 3090 and 3142 Å, which were previously observed in Comet Bennett (1970 II) by the Orbiting Astronomical Observatory OAO-2 (*1*), both atomic oxygen (OI) (1304 Å) and atomic carbon (CI) (1657 and 1561 Å) were detected; the derived luminosities are commensurate with those observed by Opal *et al.* (*2*) 3 days later. No other spectral features are clearly identified, from either the coma or the tail.

The payload consisted of two scanning Ebert spectrophotometers, each with an off-axis paraboloid of 50-cm focal length which focused the image of the comet on the entrance slit. One spectrometer, with a focal length of 25 cm, covered the wavelength range from 1200 to 1700 Å at a resolution of 10 Å with an effective field of view of 7 by 35 arc minutes. The other, with a 12.5-cm focal length, monitored the spectral region from 1800 to 3200 Å at a resolution of 15 Å with a field of view of 3.5 by 21 arc minutes. In both cases, the long axis of the slit was oriented perpendicular to the sun-comet line. A CaF_2 filter was used to reduce the sensitivity of the short-wavelength spectrometer at 1216 Å by a factor of ≈ 100 in order to prevent instrumental scattering of the strong Lyman α signal from masking spectral features at the limit of detectability. A Nikon F camera with a programmed motor drive and a lens with a focal length of 180 mm was included for aspect information.

Spectral data are shown in Fig. 1. The short-wavelength spectrum is shown on an expanded vertical scale and is the sum of all the data obtained with

Table 1. Ultraviolet emissions from Comet Kohoutek (1973f). Abbreviations: λ, wavelength; F, flux; L, luminosity; g, emission rate factor (at 1 A.U.); τ, lifetime (at 1 A.U.); and Q, production rate.

Species	λ (Å)	F (photon sec^{-1} cm^{-2})	L (photon sec^{-1})	g (photon sec^{-1} mol^{-1})	τ (sec)	Q (sec^{-1})
OI	1304	120 ± 40	2.8×10^{29}	5.0×10^{-7}*	4.0×10^{6}	1.4×10^{29}
CI	1657	140 ± 50	3.3×10^{29}	1.1×10^{-5}*	2.5×10^{6}	1.2×10^{29}
OH	3090	3100 ± 100	7.4×10^{30}	1.2×10^{-3}*	7.9×10^{4}	0.8×10^{29}
CO	1510	≤ 15	$\leq 4 \times 10^{28}$	8.2×10^{-8}	6.9×10^{5}	$\leq 7.1 \times 10^{29}$
CO_2	2890	≤ 18	$\leq 4 \times 10^{28}$	9.1×10^{-8}	3.9×10^{6}	$\leq 1.1 \times 10^{30}$
HI	1216			2.1×10^{-3}		5.4×10^{29}
				5.2×10^{-3}†		2.2×10^{29}†

* A Doppler shift of 55 km sec^{-1} was allowed for. † Derived by using the solar Lyman α flux of Keller and Thomas (*11*).

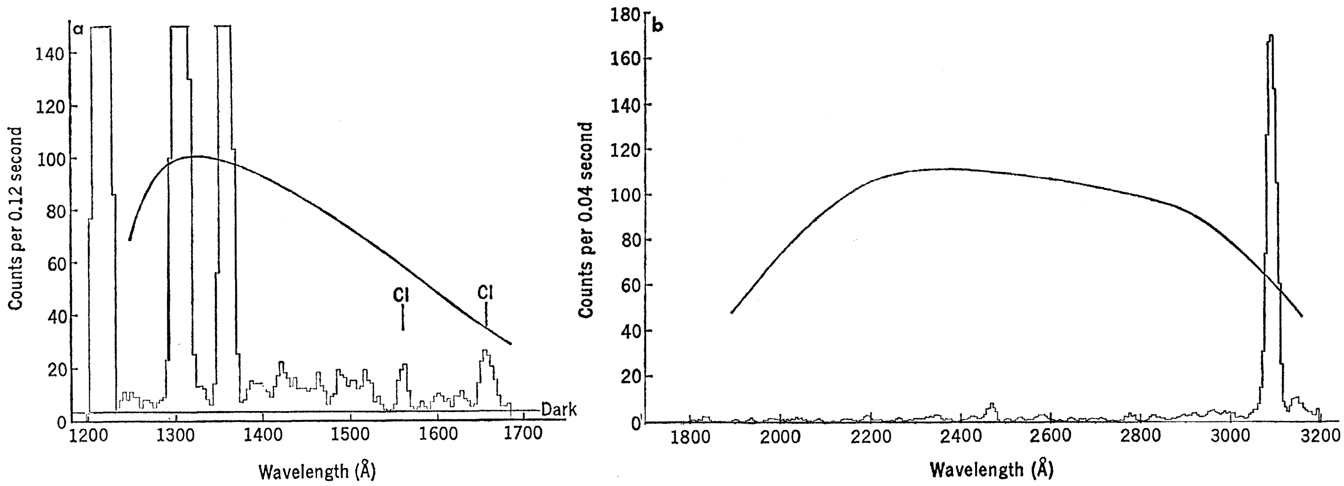

Fig. 1. Ultraviolet spectra of Comet Kohoutek (1973f) obtained on 5.1 January 1974 U.T. (a) Sum of all spectral scans from the short-wavelength spectrometer. The vertical scale is expanded to emphasize the CI lines identified in the figure. The dark count level and the instrumental response to a source of uniform intensity are indicated. (b) Long-wavelength spectrum obtained at $\approx t + 193$ seconds, showing the OH bands at 3090 and 3142 Å. The dark count level is negligible on the vertical scale.

the rocket telescope pointed in the vicinity of the comet. The off-scale features are HI Lyman α (1216 Å) from the comet and the OI lines at 1304 and 1356 Å. All the 1356-Å and most of the 1304-Å radiation is from the earth's airglow. The CI resonance lines at 1561 and 1657 Å are indicated and are clearly identifiable in Fig. 1. In Fig. 2, which is a plot of the total counts in a particular spectral line as a function of time after launch, the enhancement of the oxygen 1304-Å count rate above the airglow emission at $\approx t + 193$ seconds, when Lyman α and CI also show maxima, represents the contribution from the comet. The forbidden 1356-Å line, not shown in Fig. 2, does not exhibit this enhancement. Photographs from the aspect camera corroborate that the image of the cometary coma was within the field of view of the spectrometers during this observation period.

The long-wavelength spectrum shown in Fig. 1 was obtained at the same time and is the only observation of the OH bands obtained during the flight. Both the (0, 0) and (1, 1) bands of the ($A^2\Sigma^+ - X^2\Pi$) transition at 3090 and 3142 Å were observed, and their intensity ratio was found to be 18 ± 3. The weaker features in the spectrum are present at all times in the flight and can be accounted for as twilight airglow emissions from NO and O_2. The CO_2^+ doublet ($\tilde{B}^2\Sigma^+ - \tilde{X}^2\Pi$) at 2890 Å, one of the strongest features in the ultraviolet dayglow of Mars (*3*) and an indicator of the presence of CO_2, is not observed.

The observed flux F and luminosity

$$L = 4\pi\Delta^2 F$$

(where Δ is the earth-comet distance) for OI, CI, and OH, and upper limits for CO_2^+ and the fourth positive system of CO, are given in Table 1. These were derived by assuming that the image of the comet at each wavelength falls completely within the spectrometer slit. The 1304- and 1657-Å images of Opal *et al.* (*2*) indicate an extent of ~ 10 arc minutes, in which case the numbers

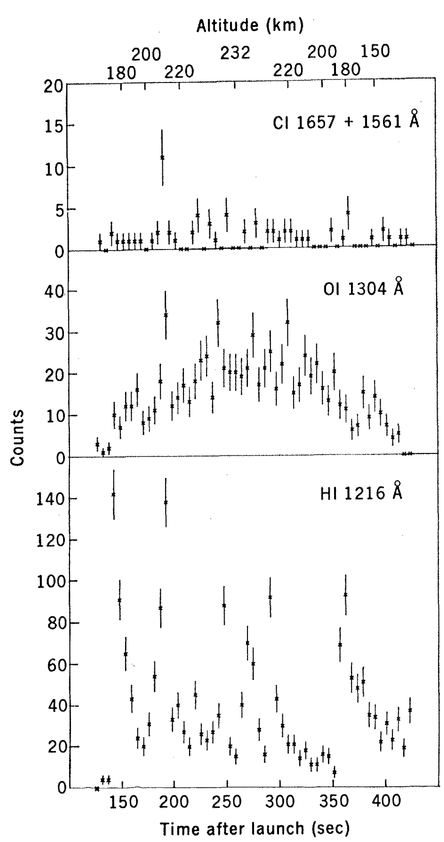

Fig. 2. Integrated counts in the resonance lines of HI, OI, and CI as a function of time after launch.

given in Table 1 represent lower limits to the actual luminosity of the comet. At the time of launch the sun-comet distance, r, was 0.34 A.U. and Δ was 0.91 A.U. The comet velocities with respect to the sun and the earth were 55 km sec^{-1} and -37 km sec^{-1}, respectively.

In order to derive the production rate, Q, of each species, we assume that the only excitation processes possible in the coma are those induced by solar radiation. Collisions within the coma and excitation by solar wind particles are neglected. For resonance scattering and resonance fluorescence, the luminosity is related to the total number of atoms or molecules, N, through the emission rate factor (*4*), g, by

$$L = gN$$

In terms of the lifetime, τ, we have

$$Q = \frac{N}{\tau} = \frac{4\pi\Delta^2 F}{g\tau}$$

The lifetime is given by $\tau = (J_i + J_d)^{-1}$, where J_i is the photoionization rate (*5*) and J_d is the photodissociation rate (*6*) (for molecules). Ionization by charge exchange with the solar wind has been neglected since the depth of penetration of the solar wind into the coma is uncertain. At most, this would reduce the lifetimes of oxygen and carbon by a factor of 2, and not appreciably affect the lifetimes of the molecules (*5*). At heliocentric distance r, $g = g_E r^{-2}$ and $\tau = \tau_E r^2$, where τ_E and g_E are values at 1 A.U., so that $g\tau = g_E \tau_E$.

The large Doppler shift at the time of observation precludes the use of "standard" emission rate factors in the calculation of Q. This is particularly severe for the OI 1304-Å triplet, where the Doppler shift, 0.25 Å, exceeds the width of the solar OI lines as recently observed at high resolution by groups from the Naval Research Laboratory (*7*) and the University of Colorado (*8*). Resonance scattering from the solar continuum and fluorescence excited by Lyman β (*9*) contribute roughly equally to the OI g-factor given in Table 1. For the CI line at 1657 Å, high-resolution solar spectra (*7*) were used to compute the g-factor given. Because of the multiplet structure of this line, the Doppler-shifted value is only reduced by a factor of 2 from the unshifted one.

The g-factors and lifetimes (*10*) at 1 A.U. adopted for this work and the derived values of the source rate Q are also given in Table 1. The error in the Q values is due principally to the uncertainties in both g-factors and lifetimes and may well exceed a factor of 2. The Q value for H, also given in Table 1, is obtained by scaling the production rate derived by Opal *et al.* (*2*) from the Lyman α isophotes and our maximum apparent Lyman α brightness of 60 kR integrated over the field of view (7 by 35 arc minutes). Alternative values for H, based on the solar Lyman α flux (average inner blue wing) derived by Keller and Thomas (*11*) from an analysis of the curvature of the Lyman α coma of Comet Bennett, are also given. The actual value of Q_H most likely lies somewhere between the two values given in Table 1.

Despite the high probable errors in the source rates given in Table 1, these results present a consistent picture of water vapor dissociation in which

$$Q_{H_2O} = Q_O = Q_{OH} = \frac{1}{2} Q_H$$

Moreover, it is clear that atomic carbon is produced at about the same rate as water vapor, and this can occur only if the parent molecule containing the carbon is evaporated at the same rate as H_2O. Delsemme (*12*) has pointed out that production rates of C_2 or CN are typically of the order of 1 percent of the water production rate for a "medium-bright" comet such as Comet Bennett, so it is unlikely that any hydrocarbon molecule is the carbon parent. This points to CO as the probable source of the carbon, and the limit on Q_{CO} set by the data on the CO fourth positive system is consistent with Q_C. While CO_2 is also a likely candidate and cannot be excluded by the data on the production rate of CO_2 set by the CO_2^+ doublet, the large strength of CO^+ bands usually observed in comet tails, relative to the strength of CO_2^+ bands, argues strongly for CO as the parent molecule. The view is further supported by the fact that CO is observed to be the second most abundant molecule, after H_2, in the interstellar medium (*13*).

PAUL D. FELDMAN
PETER Z. TAKACS
WILLIAM G. FASTIE
Physics Department, Johns Hopkins University, Baltimore, Maryland 21218
BERTRAM DONN
Astrochemistry Branch, NASA Goddard Space Flight Center, Greenbelt, Maryland 20771

References and Notes

1. A. D. Code, T. E. Houck, C. F. Lillie, *NASA SP-310* (1972), p. 109.
2. C. B. Opal, G. R. Carruthers, D. K. Prinz, R. R. Meier, *Science* **185**, 702 (1974).
3. A. Dalgarno and T. C. Degges, *Planetary Atmospheres, Proc. IAU (Int. Astron. Union) Symp. No. 40* (1971), p. 337.
4. C. A. Barth, *Appl. Opt.* **8**, 1295 (1969).
5. G. L. Siscoe and N. R. Mukherjee, *J. Geophys. Res.* **77**, 6042 (1972); W. I. Axford, *NASA SP-308* (1972), p. 609.
6. M. B. McElroy and D. M. Hunten, *J. Geophys. Res.* **75**, 1188 (1970); M. B. McElroy and J. C. McConnell, *ibid.* **76**, 6674 (1971).
7. G. E. Brueckner and K. Nicolas, *Bull. Am. Astron. Soc.* **4**, 378 (1972).
8. E. C. Bruner, Jr., R. W. Parker, E. Chipman, R. Stevens, *Astrophys J. Lett.* **182**, L33 (1973).
9. T. M. Donahue and W. G. Fastie, in *Space Research 4*, P. Muller, Ed. (North-Holland, Amsterdam, 1964), p. 304.
10. The OH lifetime is taken from measurements on Comet Kohoutek (1973f) by J. Blamont and M. Festou [*C. R. Hebd. Seances Acad. Sci. Ser. B Sci. Phys.* **278**, 479 (1974)]. The OH g-factor, allowing for a Doppler shift of 55 km sec^{-1}, is from F. Mies (private communication).
11. H. U. Keller and G. E. Thomas, *Astrophys. J. Lett.* **186**, L87 (1973).
12. A. H. Delsemme, *Space Sci. Rev.* **15**, 89 (1973).
13. D. M. Rank, C. H. Townes, W. J. Welch, *Science* **174**, 1083 (1971).
14. We wish to acknowledge the excellent support given by the Sounding Rocket Division of NASA Goddard Space Flight Center and the Naval Ordnance Missile Test Facility at White Sands Missile Range during the preparation and launch of this experiment. We thank C. B. Opal and K. Nicolas for valuable discussions. This work was supported by NASA grant NGR 21-001-001.

22 April 1974

Meteors and Meteorites Detected by Infrasound

Abstract. *The Lamont-Doherty tripartite array of microphones has detected acoustic signals from meteors. These signals yield trace velocities which vary rapidly from supersonic to nearly infinite values for successive waves or wave groups, indicating a rapidly moving source. The trajectory is constructed on the basis of an assumption of reasonable path elevations. With a second array it would be possible to obtain more positive trajectory fixes and probable ground impact locations. Initial results suggest that most acoustic meteors are meteorite-type objects rather than the low-density objects commonly detected at high elevations by photographic and radio techniques.*

The Lamont-Doherty infrasound system consists of two tripartite arrays of capacitor microphones at the same location operating in the passbands 0.1 to 1 hertz and 1 to 10 hertz, respectively. The horizontal trace velocity and the source azimuth are computed from the differences in the arrival times of the waves across each array. Many signals have been recorded which we attribute to meteoric sources.

An example of a typical signature of meteoric infrasound is shown in Fig. 1A, which indicates how such signals stand out from the background. The pressure amplitudes of the meteor signatures are about 1 μbar (1 dyne/cm^2). Figure 1B is a tape playback of the acoustic signal to a strip chart driven at high speed. Similar phases are correlated wtih broken lines. For the more common stationary acoustic sources, the slopes would be constant, indicating a constant time delay across the array. But here the slopes show a rapidly changing and decreasing time delay to nearly zero between waves 6 and 7 and then a reverse in direction with increasing delay. Such rapidly changing time delays indicate a fast-moving elevated source. For an airplane to generate the observed signal at a normal cruising elevation, about

Table 1. Data computed for waves 1 through 10 from observations of wave arrival times at the tripartite elements.

Wave number	Azimuth (deg)	Trace velocity (m/sec)	Elevation angle (deg)
1	148	391	28
2	157	500	47
3	158	600	55
4	161	650	58
5	168	840	66
6	200	990	69
7	236	1140	73
8	263	1140	73
9	274	950	68
10	290	800	65